Supporting Material

The Influenza Fusion Peptide Adopts a Flexible Flat V Conformation in Membranes

Sébastien Légaré, and Patrick Lagüe

Département de biochimie, microbiologie et bio-informatique, Institut de biologie intégrative et des systèmes (IBIS), and Centre de recherche sur la fonction, la structure et l'ingénierie des protéines (PROTEO), Université Laval, Québec (Québec) Canada

Table S1 : Total, partial and individual solvent accessible surface area (SASA) values from the equilibrated part of the trajectories, for the three peptides.

Fig. S1 : Side chains insertion depths under the phosphate groups from WT simulations compared to EPR experimental results from Han et al.(1).

Fig. S2 : Average helical fraction for the three peptides and pdb 1IBN.

Table S2 : Occurrence (%) of backbone hydrogen bonds in the kink region of the fusion peptide for the inverted-V, flat-V, hairpin and straight helix conformations. Hydrogen bonds are defined by a distance of 2.4 Å or less between the carbonyl oxygen and the amine hydrogen.

Fig. S3 : Average $^{1}H_{\alpha}$ chemical shifts differences between experimental values and SPARTA+ computed values for the F9A mutant and PDB 2JRD (top)(2), and for the W14A mutant and PDB 2DCI (bottom) (3). Experimental values taken from BMRB entries 15390 (F9A) and 6954 (W14A). The error bars are represented only for the residues with a significant difference from the experimental value. RMSDs between experimental and SPARTA+ values are of 0.156 and 0.182 ppm for F9A and W14A, compared to 0.204 and 0.250 ppm for 2JRD and 2DCI.

Fig. S4 : Distances between α protons and aromatic rings in the region of the FP kink.

Fig. S5 : Standard deviation σ of the backbone Φ dihedral angle per residue, for the three peptides.

Fig. S6, S7 and S8 : Kink angle time series for the WT, F9A and W14A peptides, respectively. The kink angle was computed with command COOR HELIX from CHARMM using residues 4-11 for the N-terminus and residues 15-18 for the C-terminus.

Fig. S9 : Kink angle θ distributions for the three peptides.

Table S1: Total, partial and individual solvent accessible surface area (SASA) values from the equilibrated part of the trajectories, for the three peptides. Standard errors in parenthesis.

SASA (Å^2)	WT		F9A		W14A	
Total	402.83	(11.90)	442.27	(10.66)	426.30	(17.52)
Residues 1-10	89.44	(5.40)	89.16	(4.51)	96.06	(6.65)
Residues 11-20	313.39	(13.64)	353.11	(13.56)	330.24	(18.82)
G1	28.78	(2.17)	25.69	(2.90)	28.65	(2.27)
L2	2.65	(0.37)	1.90	(0.22)	2.97	(0.43)
F3	4.52	(0.79)	4.64	(0.70)	5.04	(0.70)
G4	19.69	(1.75)	20.34	(0.89)	19.86	(1.75)
A5	10.06	(0.81)	9.26	(1.68)	9.80	(1.49)
I6	0.24	(0.01)	0.26	(0.01)	0.28	(0.01)
A7	6.32	(0.81)	8.86	(1.35)	8.06	(1.17)
G8	12.53	(1.47)	13.13	(1.69)	13.95	(1.44)
F/A9	3.74	(1.20)	1.62	(0.40)	4.86	(0.98)
I10	0.91	(0.24)	3.45	(1.53)	2.61	(0.87)
E11	58.62	(2.40)	72.91	(7.16)	68.65	(5.64)
N12	33.02	(2.98)	38.71	(5.74)	46.53	(3.33)
G13	0.35	(0.09)	1.30	(0.89)	1.69	(0.37)
W/A14	6.78	(0.69)	6.20	(0.70)	2.53	(0.49)
E15	80.51	(1.70)	83.18	(3.69)	75.18	(4.33)
G16	7.68	(1.21)	8.82	(1.36)	9.82	(1.54)
M17	1.06	(0.38)	1.52	(0.44)	1.49	(0.41)
I18	19.89	(1.44)	19.02	(1.19)	17.33	(3.03)
D19	74.78	(2.13)	80.46	(1.72)	78.26	(5.13)
G20	30.70	(8.36)	40.98	(8.06)	28.75	(6.00)

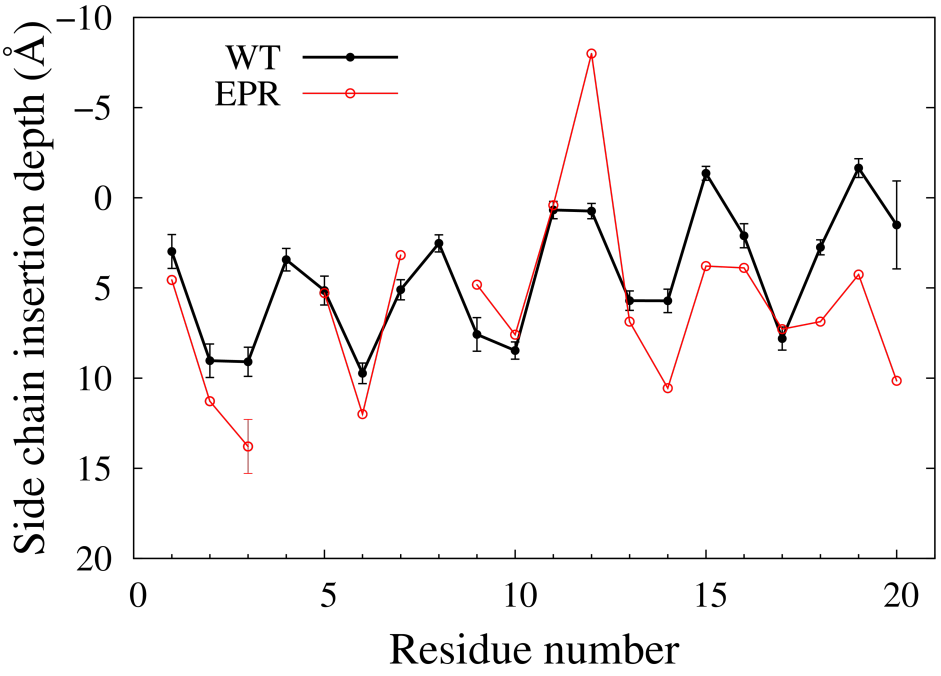

Figure S1: Side chains insertion depths under the phosphate groups from WT simulations compared to EPR experimental results from Han et al.(1).

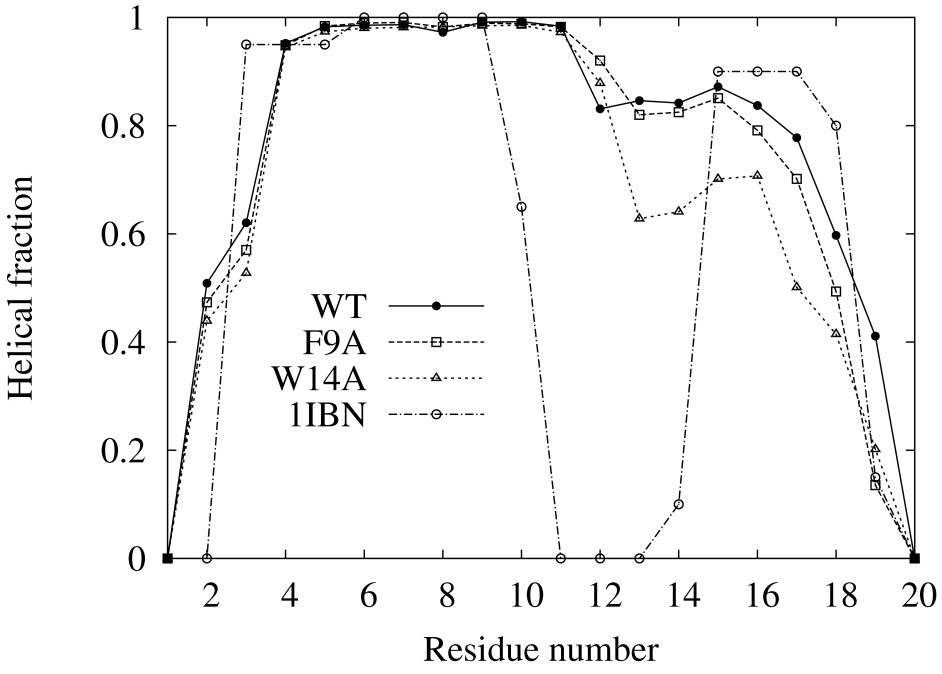

Figure S2: Average helical fraction for the three peptides and pdb 1IBN.

Table S2: Occurrence (%) of backbone hydrogen bonds in the kink region of the fusion peptide for the inverted-V, flat-V, hairpin and straight helix conformations. Hydrogen bonds are defined by a distance of 2.4 Å or less between the carbonyl oxygen and the amine hydrogen.

	Inverted-V	Kinked Flat-V			Hairpin		Straight-helix		
H-bond	1IBN	WT	F9A	W14A	F9A	W14A	WT	F9A	W14A
7 CO — HN 10	0	8	7	8	10	7	6	6	7
7 CO — HN 11	40	87	87	89	84	82	92	82	90
7 CO — HN 12	0	0	0	0	0	0	0	0	0
8 CO — HN 11	55	1	2	1	2	2	1	1	1
8 CO — HN 12	0	87	92	87	91	99	94	95	93
8 CO — HN 13	0	3	1	3	0	1	0	0	0
9 CO — HN 12	100	1	1	1	1	0	0	0	0
9 CO — HN 13	30	39	77	69	33	68	84	90	83
9 CO — HN 14	75	3	0	5	0	0	0	0	0
10 CO — HN 13	0	23	3	10	9	0	5	3	4
10 CO — HN 14	5	7	0	5	0	0	92	93	95
10 CO — HN 15	0	0	0	0	0	0	0	0	0
11 CO — HN 14	0	0	0	2	0	0	3	3	3
11 CO — HN 15	0	6	0	2	0	0	81	82	80
11 CO — HN 16	0	0	0	0	0	0	0	0	0
12 CO — HN 15	0	2	1	3	0	0	2	2	2
12 CO — HN 16	0	83	61	56	43	61	85	84	86
12 CO — HN 17	0	0	0	0	0	0	0	0	0
13 CO — HN 16	90	8	12	13	31	20	2	2	4
13 CO — HN 17	5	43	41	37	73	89	62	60	60
13 CO — HN 18	0	0	0	0	0	0	0	0	0
14 CO — HN 17	95	31	25	24	10	5	20	22	11
14 CO — HN 18	65	65	55	30	27	45	69	67	27
14 CO — HN 19	0	0	0	0	0	0	0	0	0

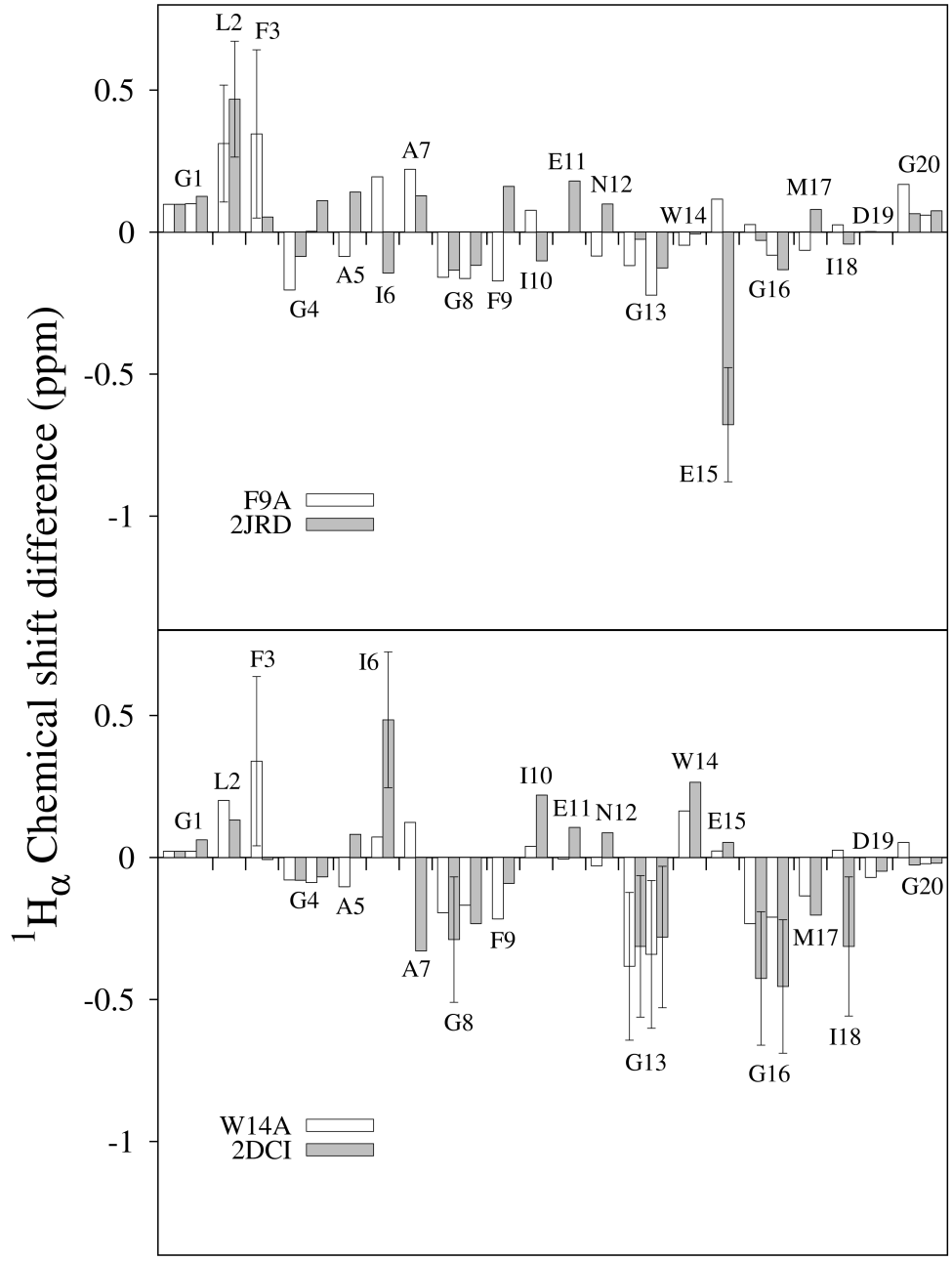

Figure S3: Average $^1H_\alpha$ chemical shifts differences between experimental values and SPARTA+ computed values for the F9A mutant and PDB 2JRD (top)(2), and for the W14A mutant and PDB 2DCI (bottom) (3). Experimental values taken from BMRB entries 15390 (F9A) and 6954 (W14A). The error bars are represented only for the residues with a significant difference from the experimental value. RMSDs between experimental and SPARTA+ values are of 0.156 and 0.182 ppm for F9A and W14A, compared to 0.204 and 0.250 ppm for 2JRD and 2DCI.

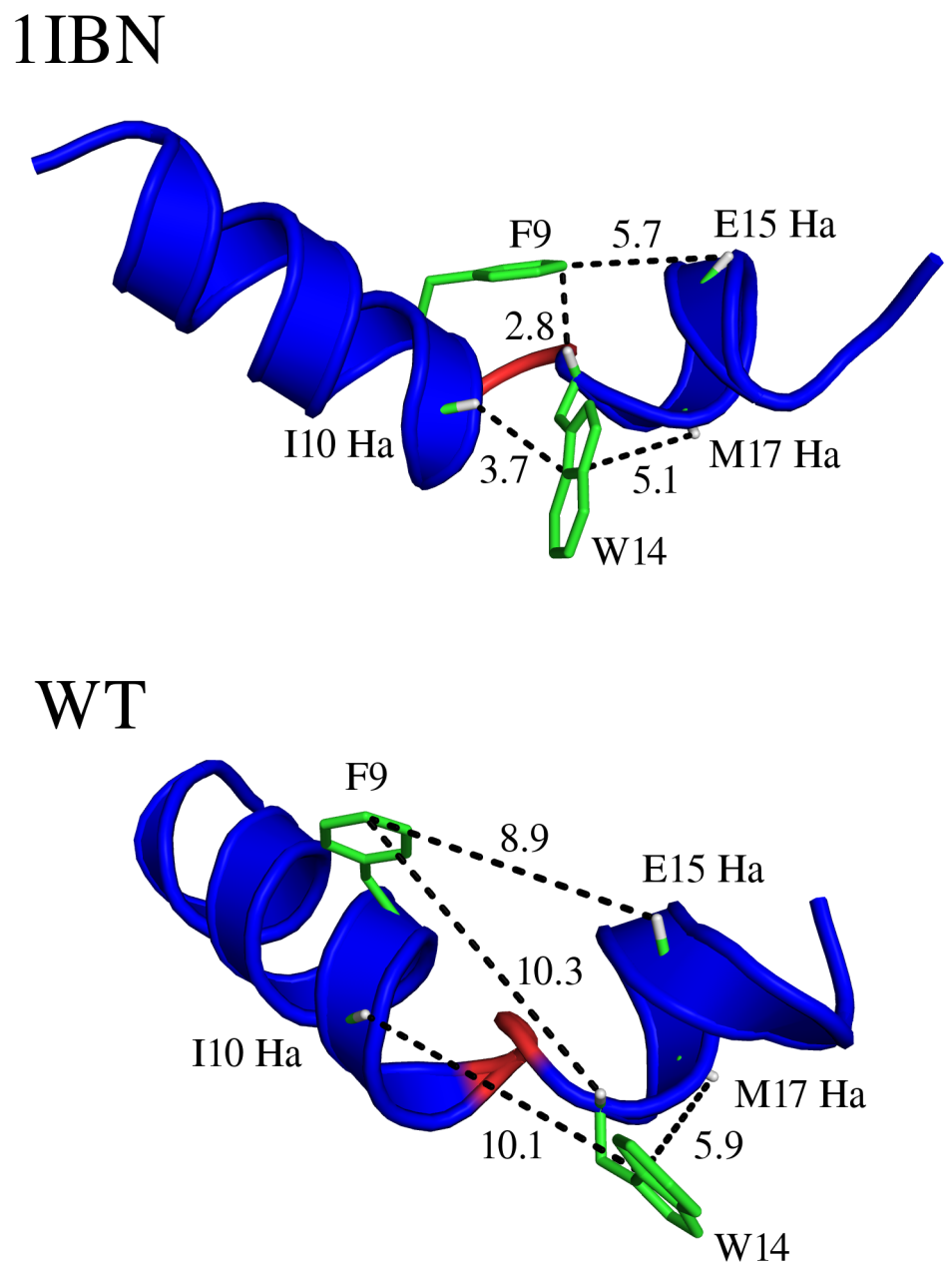

Figure S4: Distances between α protons and aromatic rings in the region of the FP kink. Distances are given in Angstroms and compared between structure 1 of pdb 1IBN and a typical kinked conformation from WT simulations.

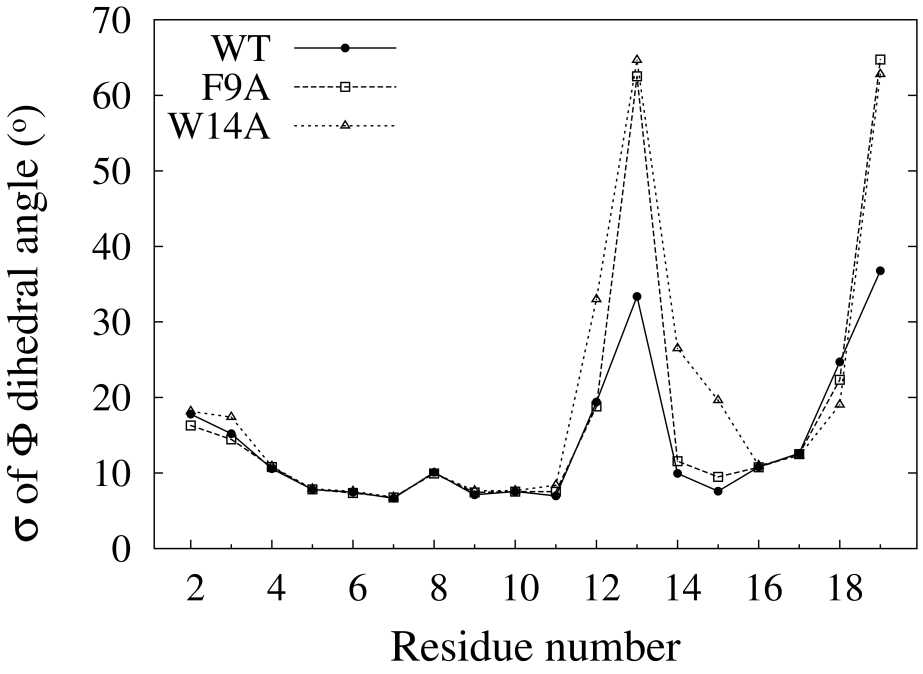

Figure S5: Standard deviation σ of the backbone Φ dihedral angle per residue, for the three peptides.

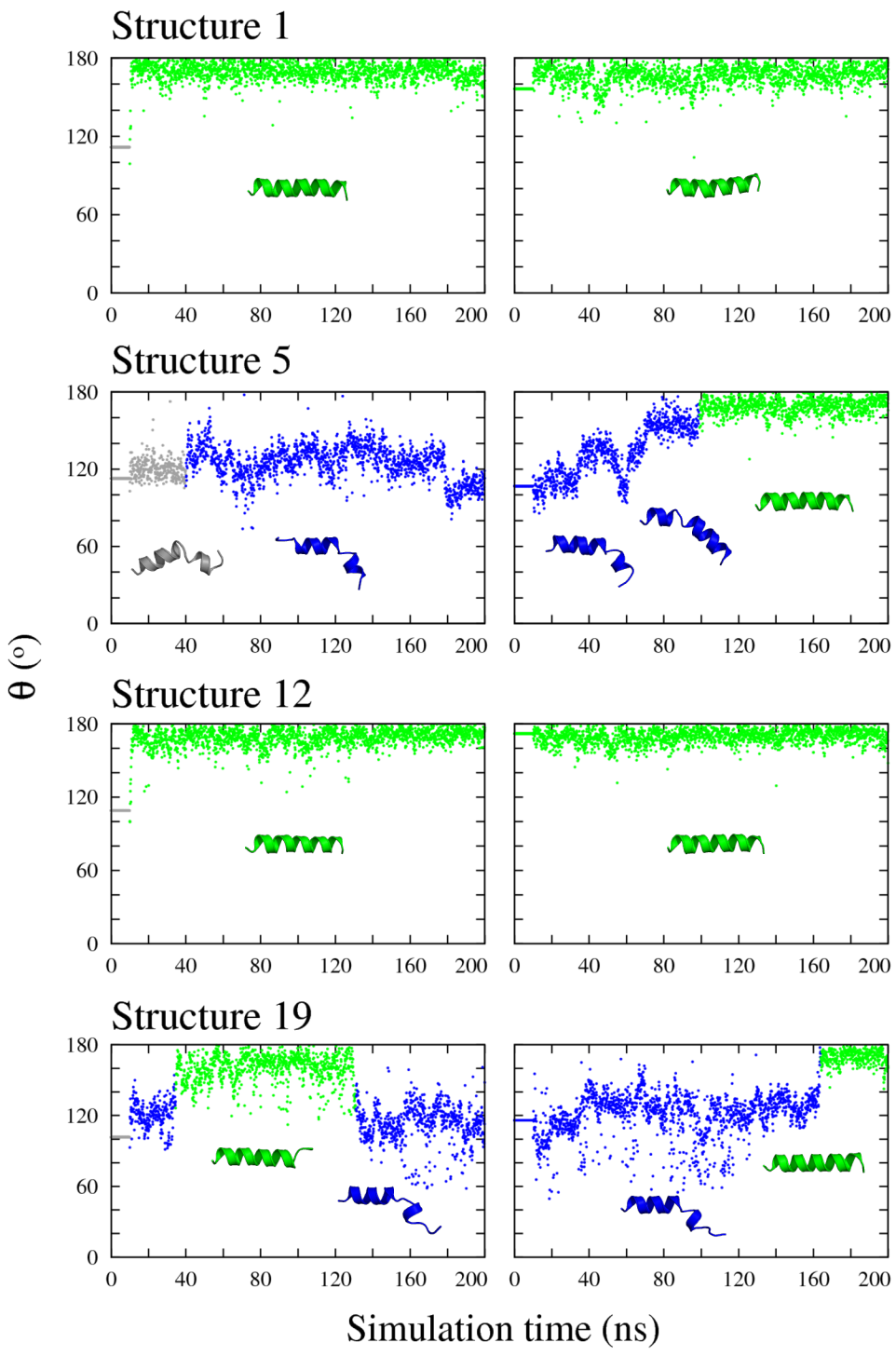

Figure S6: WT kink angle time series. For each of the four starting conformations (structures 1, 5, 12 and 19 from 1IBN), an initial 200 ns simulation (left) is performed. The final snapshot of this initial simulation is used as starting conformation for a second 200 ns simulation (right). Helical conformations are in green, kinked conformations in blue, unfolded C-terminus in red, hairpin in yellow and inverted-V in gray.

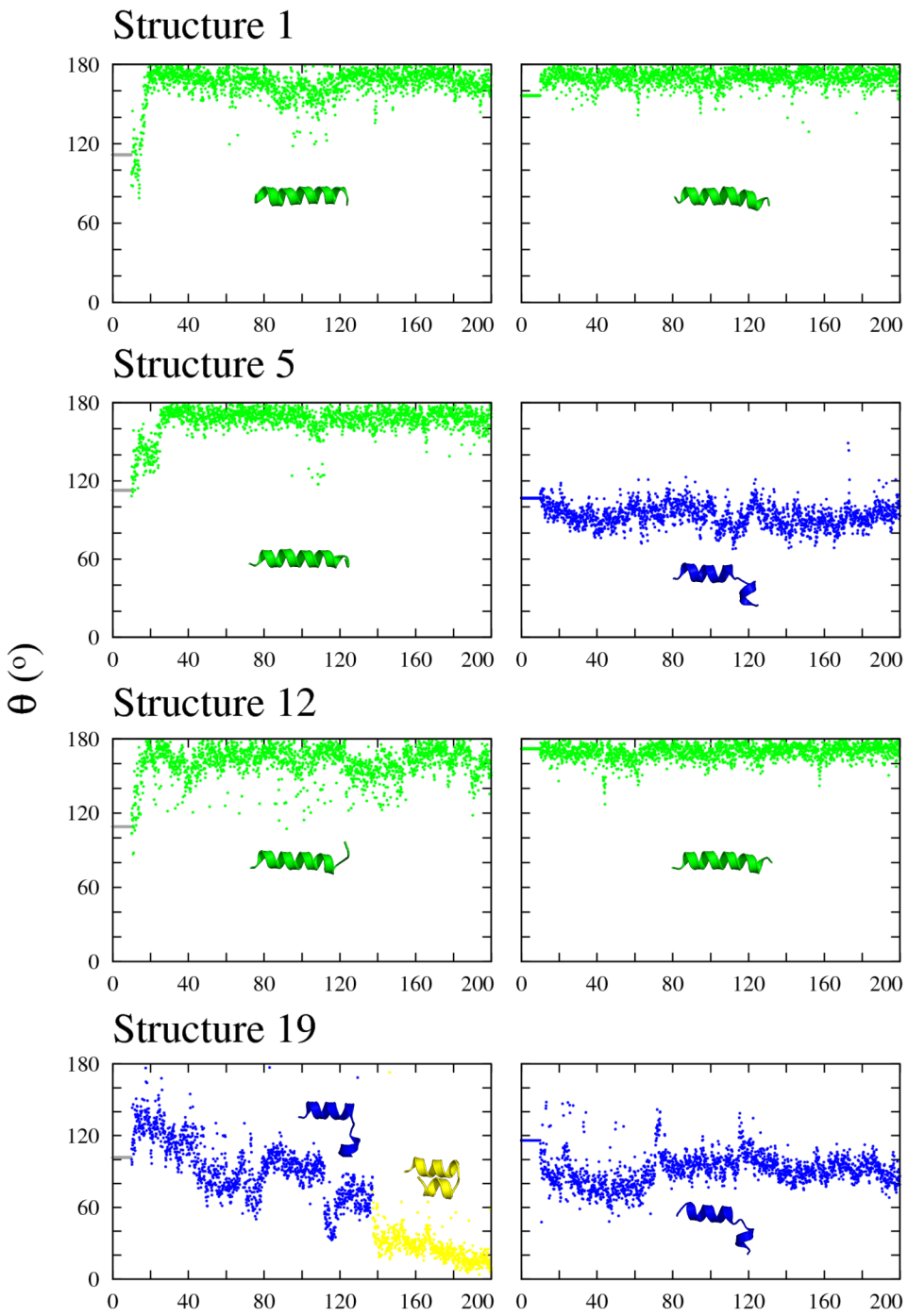

Figure S7: F9A mutant kink angle time series. For each of the four starting conformations (structures 1, 5, 12 and 19 from 1IBN), F9 is mutated to an alanine and a first 200 ns simulation (left) is performed. The final snapshot of the inital WT simulation is also mutated and used as starting conformation for a second 200 ns simulation (right). Helical conformations are in green, kinked conformations in blue, unfolded C-terminus in red, hairpin in yellow and inverted-V in gray.

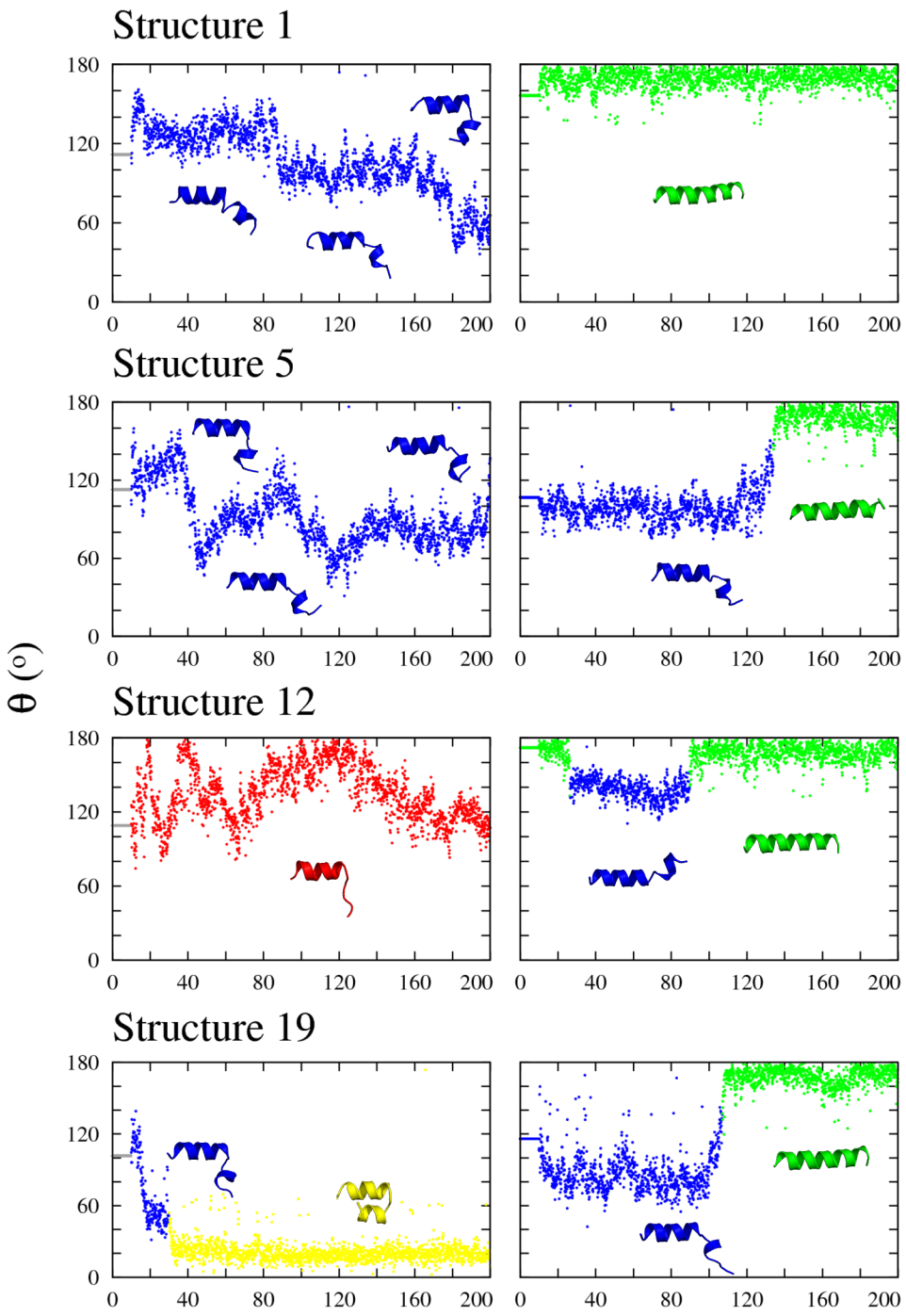

Figure S8: W14A mutant kink angle time series. For each of the four starting conformations (structures 1, 5, 12 and 19 from 1IBN), W14 is mutated to an alanine and a first 200 ns simulation (left) is performed. The final snapshot of the inital WT simulation is also mutated and used as starting conformation for a second 200 ns simulation (right). Helical conformations are in green, kinked conformations in blue, unfolded C-terminus in red, hairpin in yellow and inverted-V in gray.

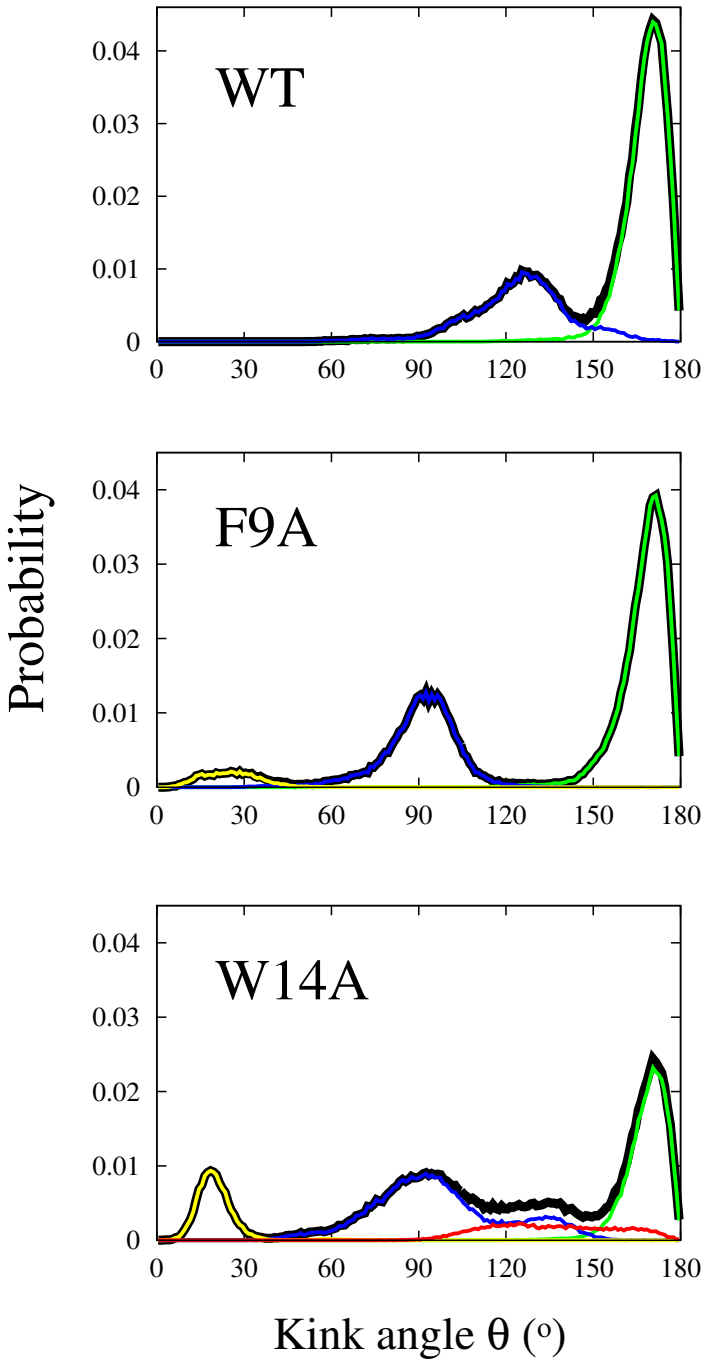

Figure S9: Kink angle θ distributions for the three peptides. Helical conformations are in green, kinked conformations in blue, unfolded C-terminus in red and hairpin in yellow. The sum of all distributions is drawn in black.

Supporting References

1. Han, X., J. H. Bushweller, D. S. Cafiso, and L. K. Tamm, 2001. Membrane structure and fusion-triggering conformational change of the fusion domain from influenza hemagglutinin. *Nat. Struct. Biol.* 8:715–720.

2. Lai, A. L., and L. K. Tamm, 2007. Locking the kink in the influenza hemagglutinin fusion domain structure. *J. Biol. Chem.* 282:23946–23956.

3. Lai, A. L., H. Park, J. M. White, and L. K. Tamm, 2006. Fusion peptide of influenza hemagglutinin requires a fixed angle boomerang structure for activity. *J. Biol. Chem.* 281:5760–5770.